



Formation of coupled three-dimensional GeSi quantum dot crystals

Y. J. Ma, Z. Zhong, Q. Lv, T. Zhou, X. J. Yang, Y. L. Fan, Y. Q. Wu, J. Zou, and Z. M. Jiang

Citation: [Applied Physics Letters](#) **100**, 153113 (2012); doi: 10.1063/1.3702883

View online: <http://dx.doi.org/10.1063/1.3702883>

View Table of Contents: <http://scitation.aip.org/content/aip/journal/apl/100/15?ver=pdfcov>

Published by the [AIP Publishing](#)

Articles you may be interested in

[Fabrication of quantum dots in undoped Si/Si_{0.8}Ge_{0.2} heterostructures using a single metal-gate layer](#)

Appl. Phys. Lett. **109**, 093102 (2016); 10.1063/1.4961889

[Dramatically enhanced self-assembly of GeSi quantum dots with superior photoluminescence induced by the substrate misorientation](#)

APL Mater. **2**, 022108 (2014); 10.1063/1.4866356

[Excitation wavelength dependent photoluminescence in structurally non-uniform Si/SiGe-island heteroepitaxial multilayers](#)

J. Appl. Phys. **111**, 114313 (2012); 10.1063/1.4729077


[SiGe quantum dot single-hole transistor fabricated by atomic force microscope nanolithography and silicon epitaxial-regrowth](#)

J. Appl. Phys. **100**, 094317 (2006); 10.1063/1.2358398

[Electroluminescence of Ge/Si self-assembled quantum dots grown by chemical vapor deposition](#)

Appl. Phys. Lett. **77**, 1822 (2000); 10.1063/1.1308526

Searching?
Trust
CiSE.



It's peer-reviewed
and appears in the
IEEE Xplore and
AIP library packages.

Formation of coupled three-dimensional GeSi quantum dot crystals

Y. J. Ma,¹ Z. Zhong,^{1,a)} Q. Lv,¹ T. Zhou,¹ X. J. Yang,¹ Y. L. Fan,¹ Y. Q. Wu,² J. Zou,² and Z. M. Jiang^{1,b)}

¹State Key Laboratory of Surface Physics, Key Laboratory of Micro and Nano Photonic Structures (Ministry of Education) and Department of Physics, Fudan University, Shanghai 200433, China

²Materials Engineering and Center for Microscopy and Microanalysis, The University of Queensland, QLD 4072, Australia

(Received 23 February 2012; accepted 27 March 2012; published online 11 April 2012)

Coupled three-dimensional GeSi quantum dot crystals (QDCs) are realized by multilayer growth of quantum dots (QDs) on patterned SOI (001) substrates. Photoluminescence spectra of these QDCs show non-phonon (NP) recombination and its transverse-optical (TO) phonon replica of excitons in QDs. With increasing excitation power, peak energies of both the NP and TO peaks remain nearly constant and the width of the TO peak decreases. These anomalous features of the PL peaks are attributed to miniband formation due to strong coupling of the holes and the emergence of quasi-optical phonon modes due to periodic scatters in ordered GeSi QDs. © 2012 American Institute of Physics. [<http://dx.doi.org/10.1063/1.3702883>]

High density and three-dimensionally (3D) ordered quantum dot (QD) arrays have been referred to as quantum dot crystals (QDCs).¹ The strong coupling among densely ordered quantum dots in QDCs may provide a path for the engineering of band structure and functionalities. Various physical phenomena, including electrostatic interactions,² localized states splitting and associated quasimolecular states,³ have been studied in coupled GeSi QD systems.

Generally, a perfectly regimented QDC can be realized, given that (i) the QDs are 3D ordered, (ii) the QDs are small and homogeneous, and (iii) the interdot spacing is small enough for strong overlap of carrier wave-functions. In 3D artificial QDCs, the QDs play a role similar to that of atoms in real crystals. The band offsets at the interfaces between the QD and the matrix in the QDC also play a role analogous to the periodic potential in real crystals. When QDs are 3D ordered and in close proximity to one another, significant carrier wave function overlap occurs. For QDs that are identical in both shape and size, the discrete energy levels of a single QD will split into extended states and emerge as 3D minibands. Moreover, coupling within QDCs leads to a drastic change in the electron density of states (DOS), compared to single dots or quantum well superlattices.^{4,5} The DOS in a QDC has a maximum peak in each miniband, which is evidently different from the delta-function-like DOS that is apparent in a random array of noninteracting QDs.

The miniband formation that is induced by coupling within QDCs has been studied theoretically in several material systems.⁴⁻⁶ Various physical properties, including enhanced light absorption,⁵ higher Hall mobility,⁷ high-temperature thermoelectricity,⁸ and negative differential conductance,⁹ have been reported in these systems. Enormous effort has been devoted to the realization of ordered GeSi QDs via patterning and lithographic techniques.^{1,10-13} However, the size and the period of the ordered QDs up to this point have been too large to investigate coupling effects

and the corresponding optoelectronic properties. Considering the compatibility with the sophisticated Si integration technology, there is a substantial motivation to investigate both the fundamental properties and the device applications of miniband formation in GeSi QDC.

In this letter, high density and 3D ordered GeSi QDCs are realized by multilayer growth of QDs on pit-patterned silicon on insulator (SOI) (001) substrates via nanosphere lithography. The QDs are arranged laterally in a hexagonal lattice with a periodicity of 100 nm. A systematic investigation of the photoluminescence (PL) spectra of this QDC is performed. Both non-phonon (NP) recombination and transverse-optical (TO) phonon replica of excitons in the QDC are observed. The nearly nonshifted PL peaks and the decrease of the full width at half maximum (FWHM) of the TO peak with increasing excitation power are examined. These characteristics are explained in terms of miniband formation due to the strong coupling of closely adjacent dots and the emergence of quasi-optical phonon modes due to periodic scatters in the QDC, respectively. Such unique features of QDCs can improve the optical properties, the carrier transportation, and the thermoelectricity, which may have promising applications in optoelectronic and thermoelectric devices.

The samples were grown by molecular beam epitaxy (MBE) on pit-patterned SOI (001) substrates, which are fabricated via nanosphere lithography.¹² The buried oxide and the top silicon layers are 370 and 30 nm thick, respectively. Polystyrene (PS) spheres of 100 nm in diameter were employed to form densely periodic PS sphere patterns on the SOI (001) substrates via self-assembly. A net-like mask composed of the Au pattern thermally evaporated between the PS spheres and the Au-catalyzed SiO₂ formed naturally. Periodic pits, arranged in the same ordering as the PS spheres, were then obtained after selective etching of the Si by a KOH solution. The pit-patterned SOI substrates were cleaned by the standard RCA method and passivated by HF prior to loading into the MBE chamber. The deposition rate of Si and Ge is 0.36 and 0.06 Å s⁻¹, respectively. The typical

^{a)}Electronic mail: zhenyangz@fudan.edu.cn.

^{b)}Electronic mail: zmjiang@fudan.edu.cn.

growth procedures are as follows. After the thermal desorption at 780 °C for 3 min, a 64-nm thick Si buffer layer was deposited at 400 °C. The first QD layer was grown by depositing 5 monolayers (MLs) of Ge with increasing the growth temperature from 450 to 550 °C. An additional 5 MLs of Ge were then deposited at 550 °C. A 5.5 nm thick Si spacer layer was deposited with increasing the growth temperature from 450 to 550 °C. The subsequent QD layers were grown at 550 °C, separated by the same Si spacer layers. To suppress enlargement of the QDs in the subsequent layers induced by strain accumulation,¹⁴ a descending of 0.5 ML Ge after every 3 layers was employed. For PL characterization, a Si cap layer of 100 nm was deposited at 400 °C. Finally, the samples were cooled down to room temperature immediately. The surface morphologies of the samples were characterized using atomic force microscopy (AFM). Cross-sectional transmission electron microscopy (XTEM) images were also obtained from a sample of ten-layer ordered QDs with the same growth parameters. For PL measurements, the samples were placed in a closed-cycle helium cryostat with a temperature range from 16 K to room temperature. An Ar⁺ laser (488 nm) was used as the excitation source. The PL spectra were recorded by an extended InGaAs detector using the standard lock-in technique.

Figure 1(a) shows the surface morphology of the pyramid shaped GeSi islands that nucleated in the ordered nanopits on a pit-patterned SOI (001) substrate. The uniform GeSi islands are arranged in a hexagonal lattice with a periodicity of 100 nm. Lateral ordering of the QDs are maintained after fifteen-layer stacking, as shown in Fig. 1(c). Based on statistical analyses of the QD height, shown in Fig. 1(d), the mean height of the GeSi QDs in the fifteenth-layer (topmost) was found to be 7.8 nm with a standard dispersion of 10%. The vertical ordering can be verified by the XTEM image

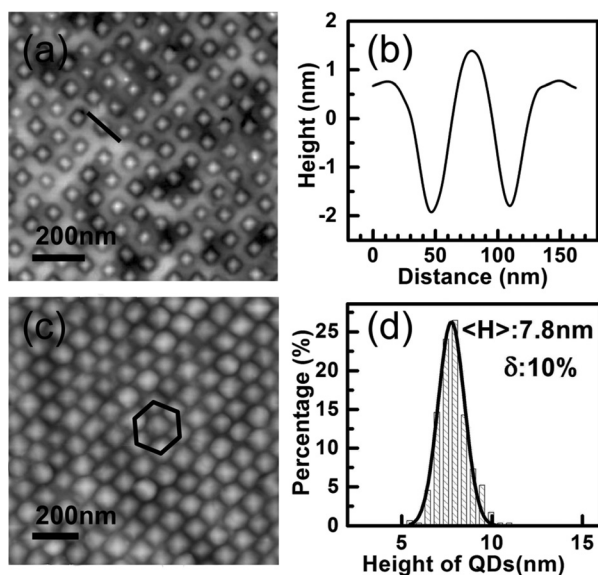


FIG. 1. (a) AFM image of the ordered pyramid shaped QDs in the first layer of the QDC (bottommost layer of QDs). (b) Height profile along the line shown in (a). (c) AFM image of the ordered QDs in the fifteenth-layer of the QDC (topmost layer of QDs). (c) The hexagonal ordering is schematically illustrated by a hexagon. (d) Statistical height distribution of the ordered QDs shown in (c), the average value (H) and the standard dispersion δ of the height of QDs are also shown.

shown in Fig. 2, which is obtained from a sample of ten-layer uncapped QDs grown on a patterned substrate with the same growth parameters. From Fig. 2(a), the in-plane interdot spacing can be estimated to be ~ 10 nm. From the high resolution XTEM image shown in Fig. 2(b), the vertical interdot spacing and the QD height in the center-line of a QD column are found to be ~ 2.5 and ~ 4.5 nm, respectively. A schematic side view illustration of the QDC structure is illustrated in Fig. 2(c). The in-plane ordering of the QDC is predetermined only by the ordered pit-pattern on substrate while the vertical ordering is self-organized in the multilayer epitaxial process.¹ The height of the uncapped QDs in the topmost layer is larger than the QDs in the layers below. The Si capping process significantly reduces the height of the QDs due to SiGe intermixing.¹⁵ Meanwhile, trenches are formed surrounding the bottom of the QDs,¹⁶ which also enlarge the AFM measured height of the topmost QDs. Thus, densely 3D ordered GeSi QD arrays have been realized and can be referred to as QDCs. Such QDCs may allow for strong wavefunction overlap and the formation of minibands.

Figure 3(a) shows the PL spectrum of a capped fifteen-layer GeSi QDC measured at 16 K and under excitation power of 0.3 W. The PL spectrum of a capped fifteen-layer random GeSi QDs sample that was grown under the same conditions is also shown. The intensity of the PL peak for the QDC is much stronger than that for the random QDs. This result demonstrates that the optical properties of the QDC can be significantly improved compared to the random QDs. The sharp peak around 0.76 eV is related to the C-O complexes.¹⁷ The asymmetric QDC PL peak can be fitted by two Gaussian peaks, as indicated by the dash-lines in Fig. 3(a), and are separated by ~ 54 meV. Accordingly, these two peaks are assigned to be the NP peak and its TO phonon replica of QDs.¹⁸ Figure 3(b) shows the power dependence of

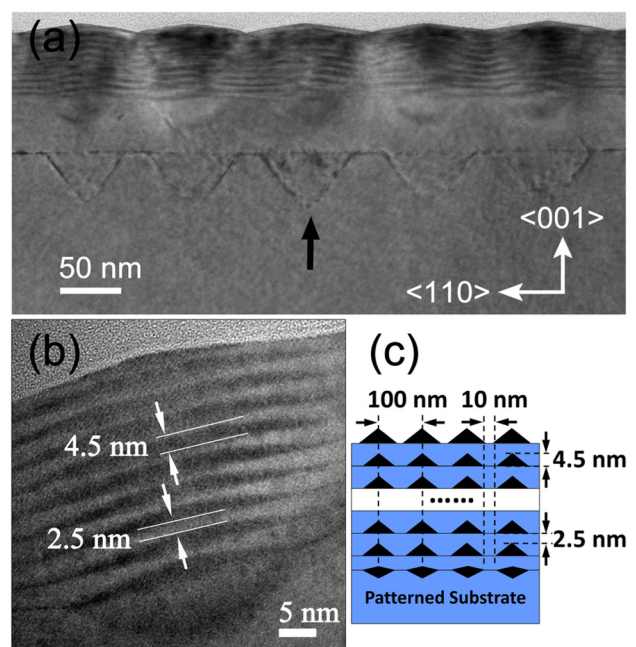


FIG. 2. (a) Cross-sectional TEM image of a ten-layer GeSi QDC. The short black arrow indicates a nanopit on the substrates. (b) HRTEM image of a QD column. (c) Schematic side view illustration of the QDC structure.

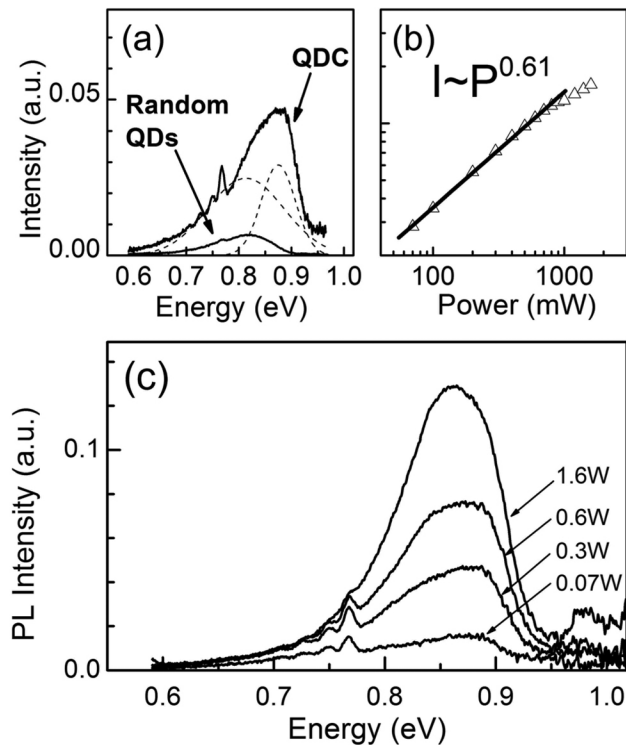


FIG. 3. (a) PL spectra of the capped fifteen-layer ordered and random QDs sample at 16 K, under excitation power of 0.3 W. The decomposed NP and TO PL peaks are indicated by dash-lines. (b) Integrated PL intensity of QDs as a function of excitation power. (c) PL spectrum of the fifteen-layer ordered QDs sample as a function of excitation power at 16 K.

integrated intensity (I_{PL}) of PL peaks of the QDC. The sub-linear relationship between the I_{PL} and the excitation power (P) is found to be $I_{PL} \sim P^{0.61}$, which indicates a typical type-II band alignment of a GeSi QD system.¹⁹ The power dependent PL spectra of the capped fifteen-layer GeSi QDC sample measured at 16 K are shown in Fig. 3(c). It is evident that the NP and TO peak energies maintain a nearly constant value of 872 (± 3 meV) and 818 meV (± 3 meV), respectively, as shown in Fig. 4(a). Such features are significantly different from previously reported PL spectra obtained from GeSi QDs with the type-II band alignment, which show a large blueshift with increasing excitation power.^{18–21}

We attribute such anomalous PL features to the formation of minibands in our GeSi QDC samples due to the strong interdot coupling. Considering the much higher band offset for heavy holes inside the QDs compared to electrons localized in the Si matrix around the QDs, it can be assumed that the minibands are mainly formed in the valence band.^{4,5,22} Theoretical results demonstrate that (i) the miniband structures of the QDCs are more sensitive to the dot regimentation rather than to the dot shape or size and (ii) the DOS will significantly increase in minibands.⁴ In our QDC sample, the QDs are 3D ordered and uniform. Accordingly, the ground state miniband of heavy holes in the valence band formed in our GeSi QDC exhibits a much higher DOS. Considering the excitation power used in the experiments, we propose that all the photo-generated holes will only partially fill in the ground state miniband. Moreover, the DOS of the miniband has a maximum value near the low-energy edge of the miniband.⁴ Thus for a weak excitation power, the photo-

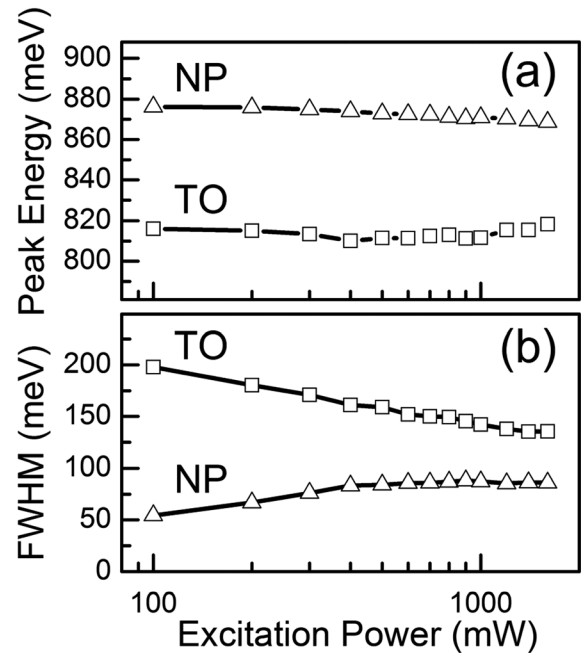


FIG. 4. (a) The peak energy, (b) the FWHM of the NP, and the TO peaks of QDs as a function of excitation power.

generated holes will fill this state of maximum density, which predominantly determines the peak energy. Consequently, in the range of the present excitation power, the shift of the PL peaks of the QDC with the excitation power is too small to be explicitly observed. Such miniband formation can also contribute to the enhanced PL efficiency for the QDC sample, as shown in Fig. 3(a).

The FWHM of the NP peak is slightly increased due to the filling effect. Generally, the FWHM of the TO replica should maintain a power dependence similar to that of the NP peak.^{18,21} However, in our QDC sample, the FWHM of the TO replica shows a much different power dependence, as shown in Fig. 4(b). According to the theoretical calculation by Lazarenkova *et al.*,⁴ many quasioptical phonon branches can emerge in QDCs due to periodic scatters, such as quantum dot boundaries. The emergence of quasioptical phonons may dramatically modify the carrier energy relaxation processes in the QDC structures. Thus, we attribute the decrease of the FWHM of the TO replica with excitation power to be the effect of quasioptical phonon emergence in our QDC sample. Further theoretical study and experiments are needed to understand this phenomenon thoroughly. Moreover, extended electron states and minibands have already been observed in partially ordered and inhomogeneous quantum dot superlattices.⁹ The formation of minibands may improve the optical properties of regimented QDs and change charge transfer in QD structures, increasing carrier mobility. The emergence of quasioptical phonon modes may dramatically affect carrier energy relaxation processes in QDC. Such unique features of QDC may stimulate their application in some optoelectronic and thermoelectric devices.

In addition, due to the limited number of coupled QDs along the growth direction, the miniband mainly extends in-plane for holes. The photo-generated electrons are mainly localized in the Si matrix above and below the QDs, a region

which is essentially not affected by miniband formation. Accordingly type-II band alignment occurs, which results in sublinear power dependence of the PL intensity, as shown in Fig. 3(b). The TO replica peak is also observed because the indirect band gap in momentum space for the Si/Ge system is not considerably changed.

In summary, we have realized high density and 3D ordered GeSi QD arrays on pit-patterned SOI (001) substrates via nanosphere lithography. Considering the excellent regimentation and the size uniformity of these ordered QDs, we refer to them as GeSi QDCs. Considerably stronger PL peaks in QDCs, compared to those of random QDs, are observed. Furthermore, with the increase of excitation power, the anomalous PL features reveal nearly constant peak energy and the FWHM of the TO replica peaks decrease. The former is explained by the miniband formation due to the strong coupling among QDs in the QDC. The latter is attributed to the emergence of quasioptical phonon modes related to the periodic scatters in the QDC. The formation of minibands and the emergency of quasioptical phonon modes in the GeSi QDC can significantly improve the physical properties of regimented QDs, which may have promising applications in some optoelectronic devices.

This work was supported by the special funds for the Major State Basic Research Project (No. 2011CB925601 and 2009CB929300) of China, Australian Research Council and the Natural Science Foundation of China (NSFC) under Project No. 10974031. Y. J. Ma also thanks the support from Fudan University by the Research Support Project for Outstanding Ph.D. Students.

¹D. Grützmacher, T. Fromherz, C. Dais, J. Stangl, E. Müller, Y. Ekinici, H. H. Solak, H. Sigg, R. T. Lechner, E. Wintersberger, S. Birner, V. Holý, and G. Bauer, *Nano Lett.* **7**, 3150 (2007).

- ²M. Manoharan, Y. Tsuchiya, S. Oda, and H. Mizuta, *Appl. Phys. Lett.* **92**, 092110 (2008).
- ³C. B. Li, G. Yamahata, J. S. Xia, H. Mizuta, S. Oda, and Y. Shiraki, *Electron. Lett.* **46**, 940 (2008).
- ⁴O. L. Lazarenkova and A. A. Balandin, *Phys. Rev. B* **66**, 245319 (2002).
- ⁵Q. Shao, A. A. Balandin, A. I. Fedoseyev, and M. Turowski, *Appl. Phys. Lett.* **91**, 163503 (2007).
- ⁶S. Rodriguez-Bolivar, F. M. Gomez-Campos, A. Luque-Rodriguez, J. A. Lopez-Villanueva, J. A. Jimenez-Tejada, and J. E. Carceller, *J. Appl. Phys.* **109**, 074303 (2011).
- ⁷Y. Bao, A. A. Balandin, J. L. Liu, J. Liu, and Y. H. Xie, *Appl. Phys. Lett.* **84**, 3355 (2004).
- ⁸T. C. Harman, P. J. Taylor, T. L. Spears, and M. P. Walsh, *J. Electron. Mater.* **29**, L1 (2000).
- ⁹H. Z. Song, K. Akahane, S. Lan, H. Z. Xu, Y. Okada, and M. Kawabe, *Phys. Rev. B* **64**, 085303 (2001).
- ¹⁰Z. Zhong, W. Schwinger, F. Schäffler, G. Bauer, G. Vastola, F. Montalenti, and L. Miglio, *Phys. Rev. Lett.* **98**, 176102 (2007).
- ¹¹Y. R. Chen, C. H. Kuan, Y. W. Suen, Y. H. Peng, P. S. Chen, C. H. Chao, E. Z. Liang, C. F. Lin, and H. C. Lo, *Appl. Phys. Lett.* **93**, 083101 (2008).
- ¹²P. X. Chen, Y. L. Fan, and Z. Y. Zhong, *Nanotechnology* **20**, 095303 (2009).
- ¹³E. Lausecker, M. Brehm, M. Grydlik, F. Hackl, I. Bergmair, M. Mühlberger, T. Fromherz, F. Schäffler, and G. Bauer, *Appl. Phys. Lett.* **98**, 143101 (2011).
- ¹⁴G. Capellini, M. D. Seta, C. Spinella, and F. Evangelisti, *Appl. Phys. Lett.* **82**, 1772 (2003).
- ¹⁵C. Lang, S. Kodambaka, F. M. Ross, and D. J. H. Cockayne, *Phys. Rev. Lett.* **97**, 226104 (2006).
- ¹⁶X. Z. Liao, J. Zou, D. J. H. Cockayne, J. Qin, Z. M. Jiang, X. Wang, and R. Leon, *Phys. Rev. B* **60**, 15605 (1999).
- ¹⁷S. Pizzini, M. Guzzi, E. Grilli, and G. Borionetti, *J. Phys.: Condens. Matter* **12**, 10131 (2000).
- ¹⁸J. Wan, G. L. Jin, Z. M. Jiang, Y. H. Luo, J. L. Liu, and K. L. Wang, *Appl. Phys. Lett.* **78**, 1763 (2001).
- ¹⁹M. W. Dashiell, U. Denker, and O. G. Schmidt, *Appl. Phys. Lett.* **79**, 2261 (2001).
- ²⁰Y. W. Chen, B. Y. Pan, T. X. Nie, P. X. Chen, F. Lu, Z. M. Jiang, and Z. Zhong, *Nanotechnology* **21**, 175701 (2010).
- ²¹C. Dais, G. Müssler, H. Sigg, T. Fromherz, V. Auzelyte, H. H. Solak, and D. Grützmacher, *Europhys. Lett.* **84**, 67017 (2008).
- ²²D. L. Nika, E. P. Pokatilov, Q. Shao, and A. A. Balandin, *Phys. Rev. B* **76**, 125417 (2007).